TITLE: CLIMATE RESEARCH
VOLUME/ISSUE/PAGES: 69 / 2 143-154
DATE: 2016
AUTHOR OF ARTICLE: LUO Q
TITLE OF ARTICLE: PERFORMANCE OF AGRO-CLIMATE INDICES AND WHEAT GRAIN YIELD IN A CHANGING CLIMATE
ISSN: 1616-1572

VA

Texas A&M University Interlibrary Loan
RAPID:LT1

ILLiad TN: 3295036

Borrower: RAPID:LT1

Lending String:

Patron:

Journal Title: Climate research

Volume: 69 **Issue:** 2
Month/Year: 2016 **Pages:** 143-154

Article Author: LUO Q

Article Title: PERFORMANCE OF AGRO-CLIMATE INDICES AND WHEAT GRAIN YIELD IN A CHANGING CLIMATE

Imprint:

ILL Number: -11927490

5/22/2017 8:26 AM
(Please update within 24 hours)

Call #: QC851 .C42

Location: stk

Scan
Charge
Maxcost:

Shipping Address:
NEW: Blake Library

Fax:
Ariel:
Email:
Odyssey: 129.82.28.195

Note:

Vol. 69: 143–154, 2016
doi: 10.3354/cr01400

CLIMATE RESEARCH
Clim Res

Published online June 27

Performance of agro-climate indices and wheat grain yield in a changing climate

Qunying Luo*

Plant Functional Biology and Climate Change Cluster, University of Technology Sydney, Sydney 2007, Australia

ABSTRACT: This study aimed to assess the performance of 8 agro-climate indices and wheat yield in 2030 and 2050 at 3 locations (Moree, Dubbo and Wagga Wagga) on a north–south climatic gradient in eastern New South Wales, Australia, by coupling downscaled outputs of 4 climate models with a mechanistic wheat model. These locations represent the transition of grain production systems from those with summer-dominant to those with winter-dominant rainfall. Simulation showed (1) ambiguous results in the frequency changes of frost occurrence across locations, phenophases, study period and sowing times; (2) a substantial increase in the frequency of heat stress during the flowering period across sowing times, study periods and locations; (3) a decrease in pre- and post-flowering rainfall in most cases; (4) no change in soil water deficit (SWD) in 2030 in 31 out of 42 cases (the combination of 7 sowings, 2 phenophases and 3 locations) and a decrease (by 0.2) or no change in SWD in 2050 in 18 out of 42 cases; and (5) a decrease, increase, or absence of change in wheat yield depending on locations, with sowing times in 2030 increasing more or decreasing less. Changes in wheat grain yield reflected the changing patterns of agro-climate indices. The concurrent occurrence of heat stress and terminal drought at wheat reproductive stages will pose significant challenges for sustainable development of the wheat industry in the future.

KEY WORDS: Wheat · Climate change · Frost risk · Heat stress · Soil water deficit · Flowering · Grain filling

1. INTRODUCTION

Frost, heat stress and soil moisture stress at reproductive stages such as flowering time and early grain filling time are common climate risks in Australian wheat production systems. Frost injury to winter grain crops, caused by extreme low temperatures (≤2.2°C, Stevenson screen temperature) at reproductive stages such as flowering time and early grain filling time, is a significant economic problem in eastern Australia, regularly causing economic losses in excess of $100 million (Fuller et al. 2007). It was estimated that the potential industry-wide payoff would be in excess of A$1 billion per year (GRDC 2014). High temperature around anthesis can substantially reduce grain yield (Wheeler et al. 2000). Half-way through anthesis (when half of the ears in a population have flowered), a temperature of ≥27°C can result in a high number of sterile grains (Wheeler et al. 1996). A maximum temperature of 35.4°C was identified as a threshold for wheat yield during the grain filling period (Porter & Gawith 1999). In southeast Australian cereal zones, the effect of high temperature is often confounded with the effect of limited water supply later in the crop growth cycle. At this time, high temperature can intensify drought impacts via increased transpiration when soil water supplies are limiting (Cawood 1996). In addition to these climate risks, growing season (GS) rainfall is an important determinant for achieving high wheat yield under rainfed and non-waterlogging conditions.

There is a growing recognition that extreme climate events such as extreme high temperature and drought will be more frequent under future climate-

*Corresponding author: luo.qunying122@gmail.com

change conditions (Cubasch et al. 2001, CSIRO & BoM 2014). This has significant implications for the wheat industry in Australia. The types of climate risk mentioned earlier need to be assessed in a changing climate. Nowadays, downscaled daily climate-change projections are available. They provide the potential to more accurately quantify the probability of exceeding extreme temperature thresholds and/or the occurrence of other climate risks based on constructed local daily climate-change scenarios, with changes both in mean climate and variability considered. Semenov (2007) quantified a drought stress index and the probability of the occurrence of hot days during wheat flowering time for Rothamsted, UK. Schlenker & Roberts (2009) quantified the effects of extreme high temperatures on USA summer crop yield in a changing climate and found that crop yield would decrease 30–46% and 63–82%, respectively, under IPCC (Intergovernmental Panel on Climate Change) B1 and A1F1 emission scenarios. Trnka et al. (2011) assessed the performance of agro-climatic indices in Europe, and concluded that rain-fed agriculture would be likely to face more climate-related risks in a changing climate. Rivington et al. (2013) quantified agro-meteorological metrics based on observed and projected climate data in Scotland, and found substantial differences between future and current situations. Based on climate indices Holzkämper et al. (2013) assessed the suitability of maize production in Switzerland under climate-change conditions. It was concluded that the positive impacts of future climate change on production conditions (i.e. optimum temperature and drought avoidance) would be counteracted by the negative impacts, such as reduced GS length and increased heat stress.

Extensive studies have been conducted regarding the climate impacts on New South Wales (NSW) wheat production (Liu et al. 2011, Potgieter et al. 2013, Luo et al. 2013, Luo & Kathuria 2013, Yang et al. 2014, Luo & Wen 2015, Ummenhofer et al. 2015). However, very limited studies have analysed climate impact on agro-climate indices and/or their ensuing effects on wheat production as illustrated below. Zheng et al. (2012) quantified the potential impacts of future frost and heat events on sowing and flowering time requirements for Australian bread wheat. Their study concluded that: (1) spatial variability would exist in frost and heat stress events, (2) sowing and flowering windows would be advanced by 2 and 1 mo, respectively, and (3) wheat GS length would be reduced especially during the pre-flowering stage. Wang et al. (2015) analysed the occurrence of the last frost and the first heat events to determine the optimal flowering date in the NSW wheat belt and identified suitable cultivars for adapting to future climate change by using a phenological framework. Innes et al. (2015) reported that high degree-hours had negative impacts on NSW wheat yield: a reduction of 5.3% for each 1°C rise in GS average daily temperature based on a statistical modelling approach. The aims of the present study were to quantify temperature- and rainfall-related risks during key phenophases of wheat crops and wheat yield under future climate conditions in the major wheat production regions of NSW, Australia, by coupling dynamically downscaled daily outputs of 4 general circulation models (GCMs) with a process-oriented wheat model through a stochastic weather generator. This study will provide useful information on the scope and identification of adaptation strategies in managing such climate risks in the economically important wheat industry.

2. METHODOLOGY

2.1. Study site

Moree, Dubbo and Wagga Wagga are located at the heart of the wheat production region in NSW, Australia. These 3 locations well represent NSW grain production areas in terms of geographical distribution, the amount of GS rainfall and their contribution to the state's wheat production. Moree belongs to the northern farming system and has a summer-dominant rainfall pattern, with GS (May through October) rainfall of 211 mm. Wagga Wagga belongs to the southern farming system and has a winter-dominant rainfall pattern, with GS rainfall of 293 mm. Dubbo is situated between Moree and Wagga Wagga, with rainfall uniformly distributed throughout the year and 252 mm of GS rainfall. Table 1 shows geographical information and the historical climate for the 3 locations considered.

Table 1. Study locations and historical climate. GST: growing season (May through October) temperature; GSR: growing season rainfall

Locations	Latitude (°S)	Longitude (°E)	Elevation (m)	GST (°C)	GSR (mm)
Moree	29.49	149.85	213	14.8	211
Dubbo	32.22	148.58	284	12.3	276
Wagga Wagga	35.05	147.35	219	10.4	293

2.2. Construction of climate scenarios

The outputs of the CSIRO Conformal Cubic Atmospheric Model (CCAM), for baseline (1980–1999) and future periods (2020–2039 [2030 period], 2040–2059 [2050 period]), were used by a stochastic weather generator (LARS-WG) to construct long (100 yr) time series of local climate scenarios, including baseline and future scenarios. Specifically, the LARS-WG was first calibrated based on historical climate datasets for the period 1980–1999. Monthly climate changes including changes in mean values (rainfall, maximum/minimum temperature and solar radiation) and variability (average length of wet/dry spells, daily and inter-annual variability of mean temperature) were then derived between future periods and baseline data. These changes were subsequently applied to the LARS-WG to construct long time series of climate scenarios based on the characteristics of historical climate derived from the aforementioned calibration process. The rationale of using this weather generator to produce climate scenarios rather than the direct use of the CCAM is that this post-processing procedure will reduce climate model error/bias. More detailed descriptions of the LARS-WG can be found in Semenov (2007) and Luo et al. (2003). The performance of the LARS-WG against observed climate has been rigorously evaluated around the world with diverse climates. It has performed well in reproducing various weather statistics including those of extreme weather events (Semenov et al. 1998, Semenov 2008). Based on the same climate model outputs used in the present study, Luo et al. (2014) evaluated the performance of the LARS-WG in NSW regions and found that LARS-WG performed reasonably well in simulating monthly mean maximum (T_{max}) and minimum (T_{min}) temperatures. The CCAM model is a variable resolution model with higher spatial resolution (15 by 15 km) in the focus area (Australia) and a coarse resolution over the rest of the globe (McGregor & Dix 2008, Luo et al. 2010, 2013). It was driven by 4 GCMs, specifically GFDL, CSIRO Mark 3.5, MPI and MIROC under the Special Report on Emission Scenarios A2 emission scenario (IPCC 2000). The rationale of using the outputs of the CCAM driven by 4 GCMs is that a multi-model ensemble is intrinsically more useful and skilful than sets of projections produced with any single model (Weigel et al. 2008). The 4 GCMs vary in their sensitivity to radiative forcing, with CSIRO Mark 3.5 being least sensitive, and MPI, most sensitive. The A2 emission scenario is the only emission scenario considered by the CCAM due to the high computing resources needed. Nonetheless it represents a relatively high-emission scenario, with correspondingly greater increases in temperature compared with other low-emission scenarios. Therefore, impact analysis based on this emission scenario should capture the upper range of possible impact.

2.3. Crop model settings and climate indices

The Agricultural Production System sIMulator (APSIM)-Wheat model (Version 7.6) was used in this study to evaluate the performance of common agro-climatic indices based on phenological dates, and to quantify wheat yield in a changing climate by coupling with climate scenarios as detailed in Section 2.2. The rationale behind using this approach is that quantified agro-climate indices are associated with actual cultivars, crop phenophases and GS length; hence, they are more realistic and accurate when compared with offline quantification in which inappropriate cultivars and phenophases, and fixed rather than cultivar- and sowing-time-dependent crop GS length, may be assumed, without consideration of relevant farm practices (i.e. matching cultivars with specific production areas and sowing timings, nor of the effects of increased temperature on crop development and GS length. This wheat model has been widely applied in several contexts worldwide, such as climate change/variability impact studies and farming system studies. Furthermore, the model has recently been modified to account for the effects of extreme temperatures on wheat production (Thorburn et al. 2013). This makes it an ideal tool for implementation in this study. More information on the APSIM can be found in the publication by Holzworth et al. (2014). The default setting of APSIM-Wheat was assumed in this analysis. O'Leary et al. (2015) evaluated the performance of the APSIM-Wheat model against 'Australian Grain Free Air CO_2 Enrichment' experimental datasets and found that simulated crop responses to enhanced CO_2 were similar/close to and within the experimental range of error for accumulated biomass, yield and water use responses. The performance of APSIM-Wheat in the NSW region was found to be very satisfactory based on district yield (https://www.apsim.info/Portals/0/NewsFeatures/DLL_Whole_farm_climate_change_2.pdf). Seven fixed sowing times were considered in this analysis starting on 1 May, with a 15 d interval, and finishing on 15 July (Table 2). The period from early May to mid-July is the typical sowing window for wheat in NSW (Matthews & McCaffery 2012). Two wheat cultivars (Sunvale and

Table 2. Sowing information

Sowing time (sowing sequence)	1 May (1)	15 May (2)	31 May (3)	15 Jun (4)	15 Jun (5)	30 Jun (6)	15 Jul (7)
Cultivar	Sunvale				Janz		
Density (plants m^{-2})	100						
Depth (mm)	30						

Janz) with different maturity dates were used in this simulation analysis. Sunvale is a mid- to late-maturing cultivar, while Janz is an early maturing cultivar. Sunvale was used in the first 4 sowings, while Janz was used in the last 3 sowings. It should be noted that the 4th (with Sunvale) and 5th (with Janz) sowing times were the same but with different cultivars, as both cultivars are possible candidates at this time (Table 2). The reason for not using both cultivars across all sowing times is that this model setting represents real farm practice. Normally cultivar choices need to match sowing times (e.g. late-maturity cultivar with early sowing). Sowing density was set to 100 plants m^{-2}, and sowing depth was set to 3 cm. A typical soil for each production area was chosen, which was obtained from APSoil, one of the toolboxes of the APSIM package. Key soil information is shown in Table 3. Nutrient management information including nitrogen and residue application is also given in Table 3. Soil water and nutrients were carried over from year to year. As mentioned in Section 2.2, 3 time periods were considered in this simulation analysis. In correspondence to these 3 timeframes, atmospheric CO_2 concentrations were set to 400, 450 and 545 ppm for baseline, 2030 and 2050 periods, respectively.

Eight climate indices were considered in this study, such as the frequency of frost and heat stress occurrence during the flowering period (FLP: from the start of flowering to the start of grain filling) and during the grain filling period (GFP, from the start of grain filling to the end of grain filling), pre- and post-flowering rainfall and soil water deficiency (SWD) for photosynthesis during the FLP and GFP. The frequency of frost occurrence was calculated as the number of days on which minimum air temperature is ≤2.2°C for both the FLP and GFP over the 100 yr climate scenarios. The reason for choosing this threshold rather than 0°C was that, under calm and clear conditions, overnight temperatures at ground level are often up to 5°C lower than those measured inside a meteorological instrument screen (Cawood 1996). The frequency of heat stress occurrence was calculated as the number of days on which maximum temperature is ≥27 and 35.4°C for FLP and GFP, respectively, over the 100 yr climate scenarios. Pre-flowering rainfall was cumulated from sowing to flowering, while post-flowering rainfall was cumulated from flowering to maturity on an annual basis. SWD (with no unit) was a direct output of the wheat model. A value of 0 corresponds to complete stress, while 1 corresponds to no stress.

Table 3. Key soil information and nutrient management information. N application (Urea-N at sowing) was 150 kg ha^{-1}. PAWC: plant available water capacity

Locations	Soil texture or type	PAWC (mm)	Initial residue (kg ha^{-1})
Moree	Clay (Vertosol)	117	1000
Dubbo	Sandy clay	134	1000
Wagga Wagga	(Sodosol)	98	1500

2.4. Comparison of agro-climate indices

To evaluate the performance of the LARS-WG, the 8 agro-climate indices derived from the APSIM-Wheat model based on observed climate (1980–1999) and baseline climate scenarios as described in Section 2.2 were compared. It should be noted that for this purpose only the 1st sowing was considered associated with the cultivar Sunvale, as an example. The focus of this study was to quantify agro-climate indices and wheat yield in a changing climate. Wilcoxon rank-sum and Kolmogorov-Smirnov tests were conducted to evaluate the mean values and distribution of rainfall-related indices, respectively. The Fisher exact test was used to determine the independence of temperature-related indices, which are counts (non-continuous data). Furthermore, the distributions of maximum temperature in October (relevant to heat stress at grain filling) and minimum temperature in September (relevant to frost risk during the flowering period) were compared between baseline data and observed climate.

3. RESULTS

3.1. Performance of the LARS-WG

Statistical test results showed that there was no significant difference in 17 out of 24 cases (the combination of rainfall-related indices, associated statistical

tests and locations) in rainfall-related indices derived from observed and modelled baseline data for the period 1980–1999 (Table 4). Overall, the distribution of rainfall-related indices performed much better than the means did, especially at Wagga Wagga. There was no significant difference in temperature-related indices derived from observed and modelled baseline data across locations (Table 4). Fig. 1 shows the distributions of maximum temperature in October and minimum temperature in September between baseline (derived from LARS-WG) and observed climate. LARS-WG underestimated the variability of both maximum temperature in October and minimum temperature in September across the 3 locations.

3.2. Local climate change in 2030 and 2050

Table 5 shows changes in the mean climate and in variability for the 2 periods and 3 locations considered, along with climate model errors. GS mean temperature is projected to increase by 1–1.3°C and 1.6–2.1°C in 2030 and 2050, respectively, across locations, with Moree experiencing the greatest increase, and Wagga Wagga experiencing the least increase (Table 5). GS rainfall is projected to decrease by –4% and from –6 to –3% in 2030 and 2050, respectively, at Moree and Dubbo, with no changes found at Wagga Wagga across the 2 future periods (Table 5). GS average length of wet spells would decrease by 3–4% in 2030 and by 4–8% in 2050 across locations. In contrast, GS average length of dry spells is projected to increase by up to 2% in 2030 and 4–5% in 2050 across locations. GS variability of mean temperature is projected to increase by 2–4% and 4–10% in 2030 and 2050, respectively, across locations. There is no error for rainfall-related variables, while an error of 0.1 is found for temperature-related variables in the majority of cases (across time periods, locations and climate variables), whether for the mean or for the variability of future climate (Table 5).

Table 4. Comparison of agro-climate indices based on observed and baseline climate for the period 1980–1999, as represented by p-values ($p \leq 0.05$: significant difference between indices derived from baseline and observed climate). Pre/PostFLR: pre-/post-flowering rainfall; SWDFL: soil water deficit at flowering; SWDGF: soil water deficit at grain filling; FrostFL: frost frequency during the flowering period; HeatFL: frequency of heat stress during the flowering period; FrostGF: frost frequency during the grain filling period; HeatGF: frequency of heat stress during the grain filling period; NA: p-value is not available because the comparison pairs do not have ≥2 levels of data; *Significant at 95% confidence level, **significant at 99% confidence level

Indices	Moree	Dubbo	Wagga Wagga
Wilcoxon rank-sum test			
PreFLR	0.1686	0.0072*	0.0225*
PostFLR	0.2629	0.2829	0.0006**
SWDFL	0.2543	0.1265	0.0268*
SWDGF	0.0198*	NA	NA
Kolmogorov-Smirnov test			
PreFLR	0.2646	0.0127*	0.129
PostFLR	0.3108	0.2646	0.0073*
SWDFL	0.5459	0.5459	1.0000
SWDGF	0.9984	1.0000	1.0000
Fisher exact test			
FrostFL	NA	1.0000	1.0000
HeatFL	0.1794	NA	1.0000
FrostGF	NA	NA	1.0000
HeatGF	NA	NA	NA

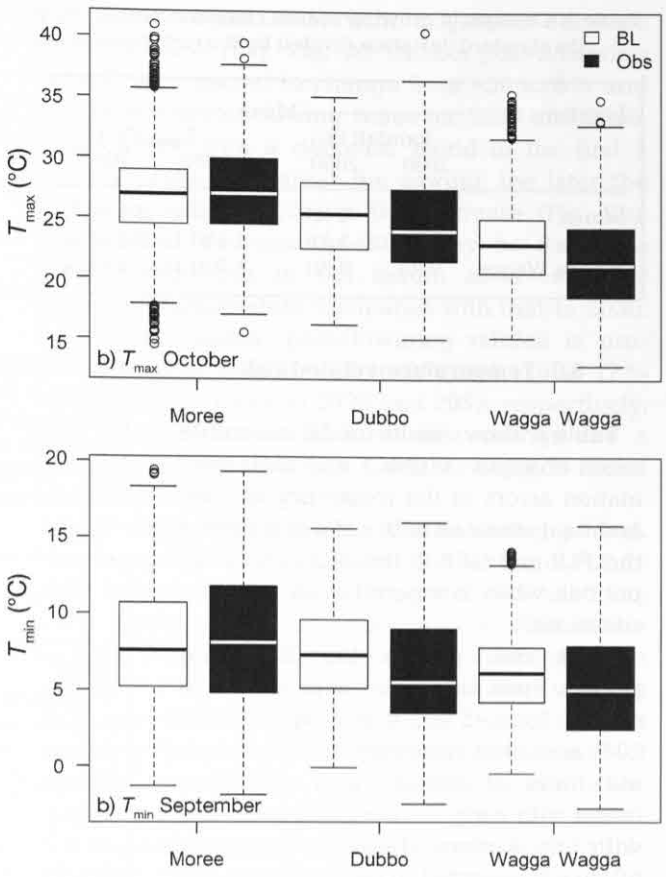

Fig. 1. Comparison of the distributions of maximum temperature in (a) October and (b) minimum temperature in September between baseline (BL; 100 yr time series, from the LARS-WG) and observed climate (Obs.; 1980–1999) across locations. Horizontal bar in box: median; lower and upper box: 25–50th and 50th –75th percentiles; lower and upper whiskers: 0–25th and 75th–100th percentiles; circles: outliers

Table 5. Changes in growing season climate across study periods and locations. Parentheses: estimation errors calculated as the standard deviation divided by the root mean square of the number of climate models. T_{mean}: mean temperature

Locations	Mean				Variability					
	Rainfall (%)		T_{mean} (°C)		Wet spells (%)		Dry spells (%)		T_{mean} (%)	
	2030	2050	2030	2050	2030	2050	2030	2050	2030	2050
Moree	−4 (0)	−6 (0)	1.3 (0.1)	2.1 (0.1)	−3 (0)	−6 (0)	0 (0)	5 (0)	2 (0.1)	4 (0)
Dubbo	−4 (0)	−3 (0)	1.2 (0.1)	2.0 (0.1)	−3 (0)	−4 (0)	2 (0)	5 (0)	3 (0.1)	10 (0.1)
Wagga Wagga	0 (0)	0 (0)	1.0 (0.1)	1.6 (0.1)	−4 (0)	−8 (0)	2 (0)	4 (0)	4 (0.1)	6 (0.1)

3.3. Temperature-related risk

Table 6 shows multi-model ensemble mean changes (MEMC) and their estimation errors in the frequency of frost and heat stress (number of days) during the FLP and GFP in the 2030 and 2050 periods when compared with baseline situations.

Frost risk during the flowering period. Frost frequency is projected to change from −5 to 2 d and −6 to 0 d for 2030 and 2050, respectively, across sowing times at Moree, with decreases found with early sowings and increases with late sowings (Table 6). Frost frequency is projected to increase by 0–6 d and 0–1 d in 2030 and 2050, respectively, at Dubbo, with an increase for early sowings (more increases in 2030) and no change for late sowings across the 2 future periods (Table 6). Frost frequency is projected to change from −10 to 0 d and −8 to 1 d across sowing times for 2030 and 2050, respectively, at Wagga Wagga. The difference in frost frequency between the 2 study periods is small (Table 6).

Heat stress during the flowering period. The frequency of heat stress is projected to increase 4–20 d and 6–26 d for 2030 and 2050, respectively, across sowing times at Moree (Table 6). Similar to Moree, the frequency of heat stress at Dubbo is projected to increase 8–23 d and 10–24 d in 2030 and 2050, respectively, across sowing times (Table 6). The frequency of heat stress at Wagga Wagga is also projected to increase (2–13 d and 1–15 d in 2030 and 2050, respectively) across sowing times. Generally speaking, the later the future

Table 6. Multi-model ensemble mean (absolute) changes (d) in the frequency of frost and heat stress during the flowering (FLP) and grain filling (GFP) periods across sowing times and locations in 2030 and 2050, compared with the baseline situation. Parentheses: estimation errors calculated as the standard deviation of a specific agro-climate index divided (from the 4 climate models) by the root mean square of the number of climate models used in this study

	Sowing						
	1	2	3	4	5	6	7
2030							
Frost during FLP							
Moree	−5 (1.8)	1 (1.3)	−2 (0.9)	−1 (0.0)	1 (0.5)	1 (0.5)	2 (1.8)
Dubbo	6 (2.3)	2 (0.9)	1 (0.5)	0 (0.0)	0 (0.0)	0 (0.0)	0 (0.0)
Wagga	−3 (2.6)	−10 (1.9)	0 (3.3)	−4 (3.3)	−2 (2.0)	−1 (2.0)	−2 (1.3)
Heat stress during FLP							
Moree	4 (1.7)	7 (5.2)	13 (6.2)	11 (5.4)	9 (5.0)	20 (4.1)	7 (5.6)
Dubbo	23 (4.3)	14 (2.5)	12 (2.9)	11 (3.4)	12 (2.9)	18 (1.5)	8 (5.6)
Wagga	5 (1.1)	3 (3.0)	13 (5.0)	2 (3.9)	4 (4.3)	7 (0.9)	2 (6.1)
Frost during GFP							
Moree	0 (1.3)	2 (0.6)	1 (0.5)	1 (0.5)	1 (0.8)	1 (1.3)	0 (0.0)
Dubbo	2 (0.9)	0 (0.3)	0 (0.0)	0 (0.0)	0 (0.0)	0 (0.0)	0 (0.0)
Wagga	−6 (2.2)	1 (3.5)	1 (2.5)	0 (1.3)	1 (0.5)	−2 (0.5)	−1 (0.0)
Heat stress during GFP							
Moree	1 (0.5)	−1 (0.0)	2 (0.6)	3 (1.4)	2 (0.6)	2 (1.0)	−3 (0.6)
Dubbo	0 (0.3)	1 (0.5)	0 (0.3)	1 (0.8)	1 (1.0)	2 (1.5)	2 (1.0)
Wagga	0 (0.0)	0 (0.0)	0 (0.3)	−2 (1.7)	−4 (1.4)	1 (0.6)	−1 (1.3)
2050							
Frost during FLP							
Moree	−6 (0.6)	−2 (0.3)	−4 (0.3)	−1 (0.0)	0 (0.0)	0 (0.0)	0 (0.0)
Dubbo	1 (1.0)	1 (0.9)	1 (0.5)	0 (0.3)	0 (0.0)	0 (0.0)	0 (0.0)
Wagga	−3 (2.8)	−8 (3.8)	1 (4.3)	−4 (3.0)	−1 (2.8)	0 (2.8)	−2 (1.3)
Heat stress during FLP							
Moree	6 (1.5)	11 (2.4)	10 (3.6)	23 (3.0)	12 (3.9)	26 (2.9)	12 (4.5)
Dubbo	24 (4.3)	22 (1.7)	12 (1.8)	13 (1.6)	16 (5.6)	20 (1.9)	10 (3.5)
Wagga	5 (1.9)	1 (3.8)	15 (4.7)	1 (5.0)	6 (3.9)	10 (1.8)	7 (1.1)
Frost during GFP							
Moree	−3 (0.5)	1 (0.9)	0 (0.3)	0 (0.0)	0 (0.0)	0 (0.0)	0 (0.0)
Dubbo	2 (1.0)	1 (0.5)	0 (0.0)	0 (0.0)	0 (0.0)	0 (0.0)	0 (0.0)
Wagga	−5 (3.0)	1 (3.5)	1 (3.0)	3 (3.5)	2 (2.0)	0 (2.0)	−1 (0.3)
Heat stress during GFP							
Moree	0 (0.3)	0 (0.4)	1 (0.5)	1 (0.7)	3 (1.5)	1 (0.4)	1 (2.1)
Dubbo	1 (0.8)	2 (1.4)	1 (1.3)	1 (1.3)	2 (2.0)	2 (1.8)	3 (1.3)
Wagga	0 (0.0)	1 (1.0)	1 (0.5)	−3 (1.3)	−5 (2.5)	0 (1.7)	1 (2.7)

period, the more the increase in the frequency of heat stress during the FLP across sowing times and locations (Table 6).

Frost risk during the grain filling period. Frost frequency is projected to change from 0 to 2 d and −3 to 1 d in 2030 and 2050, respectively, across sowing times at Moree, with no change for late sowings in 2050 (Table 6). There are no projected changes in frost frequency across sowing times or future periods at Dubbo, except the first 2 sowing times during which a small increase of 1–2 d is found (Table 6). Frost frequency is projected to change from −6 to 1 d and −5 to 3 d in 2030 and 2050, respectively, across sowing times at Wagga Wagga. The greatest decrease is found with the 1st sowing time for both future periods (Table 6).

Heat stress during the grain filling period. The frequency of heat stress is projected to change from −3 to 3 d and 0 to 3 d in 2030 and 2050, respectively, with most of the sowings showing an increase for both future periods at Moree (Table 6). The frequency of heat stress would increase 1–2 d and 1–3 d in 2030 and 2050, respectively, across sowing times at Dubbo (Table 6). The frequency of heat stress is projected to change from −4 to 1 d and −5 to 1 d across sowing times in 2030 and 2050, respectively, at Wagga Wagga (Table 6).

3.4. Rainfall-related risk

Fig. 2 shows MMEC in pre- and post-flowering rainfall and SWD during flowering and grain filling periods in 2030 and 2050 across sowing times in comparison with baseline situations.

Pre-flowering rainfall. At Moree, pre-flowering rainfall is projected to decrease from −9 to −6% and −25 to −15% across sowing times in 2030 and 2050, respectively, with a greater decrease found in 2050 (Fig. 2a). For Dubbo, pre-flowering rainfall is projected to change from −18 to 7% and −25 to 1% in 2030 and 2050, respectively, across sowing times, with later sowings showing a decrease (the later the sowing, the greater the decrease for both periods; Fig. 2a). This may be associated with the reduced GS length due to late sowing. At Wagga Wagga, pre-flowering rainfall is projected to decrease slightly (−1%) in the last 5 sowings in 2030, while it is projected to increase slightly (1–2%) in the first 6 sowings in 2050 (Fig. 2a).

Post-flowering rainfall. At Moree, post-flowering is projected to is projected to change from −15 to 2% and −33 to −26% across sowing times in 2030 and 2050, respectively, with a greater decrease found in 2050 (Fig. 2b). At Dubbo, post-flowering rainfall is projected to change from −36 to 8% and −47 to 8% across sowing times for 2030 and 2050, respectively, with a decrease found in the first 5 sowing times: the earlier the sowing, the later the future period, the greater the decrease (Fig. 2b). The greater decrease in 2050 may be due to a greater reduction in GS length as a result of increased temperature compared with that in 2030. At Wagga Wagga, post-flowering rainfall is projected to change from −16 to 8% and −29 to 17% across sowing times in 2030 and 2050, respectively, with an increase found in earlier sowings and a decrease for later sowings. Greater change is found for the 2050 period (Fig. 2b).

Soil water deficit during the flowering period. No change in SWD is projected during the FLP in 2030 at Moree. A decreased range of −0.2 to −0.1 in SWD across sowing times is found in 2050 at this location (Fig. 2c). SWD is projected to change from −0.1 to 0.1 and −0.2 to 0.1 across sowing times in 2030 and 2050, respectively, at Dubbo, with a decrease found in later sowings and a greater decrease in 2050 (Fig. 2c). This may be due to the greater increase in temperature and greater reduction in rainfall in 2050 compared with 2030 at this location. SWD is projected to increase by 0–0.1 across sowing times and the 2 future periods, with an increase for later sowings and no change for early sowings at Wagga Wagga (Fig. 2c).

Soil water deficit during the grain filling period. No change in SWD is projected during the GFP in 2030 at Moree, except for the last sowing. SWD is projected to decrease from −0.2 to 0 across sowing times in 2050 at this location (Fig. 2d). SWD is projected to change from 0 to 0.1 and −0.1 to 0.1 across sowing times in 2030 and 2050, respectively, with no change for most sowings at Dubbo (Fig. 2d). No change in SWD across sowing times and future periods is projected at Wagga Wagga (Fig. 2d).

3.5. Wheat grain yield

Average wheat yield is projected to decrease from −3 to +3% and −23 to −5% across sowing times in 2030 and 2050, respectively, at Moree, with less decrease found in 2030 compared with 2050 (Fig. 3). Wheat yield is projected to decrease from −3 to −2% and −1% in 2030 and 2050, respectively, for the first 2 sowings at Dubbo. However, wheat yield is projected to increase 30–43% and 8–34% across the

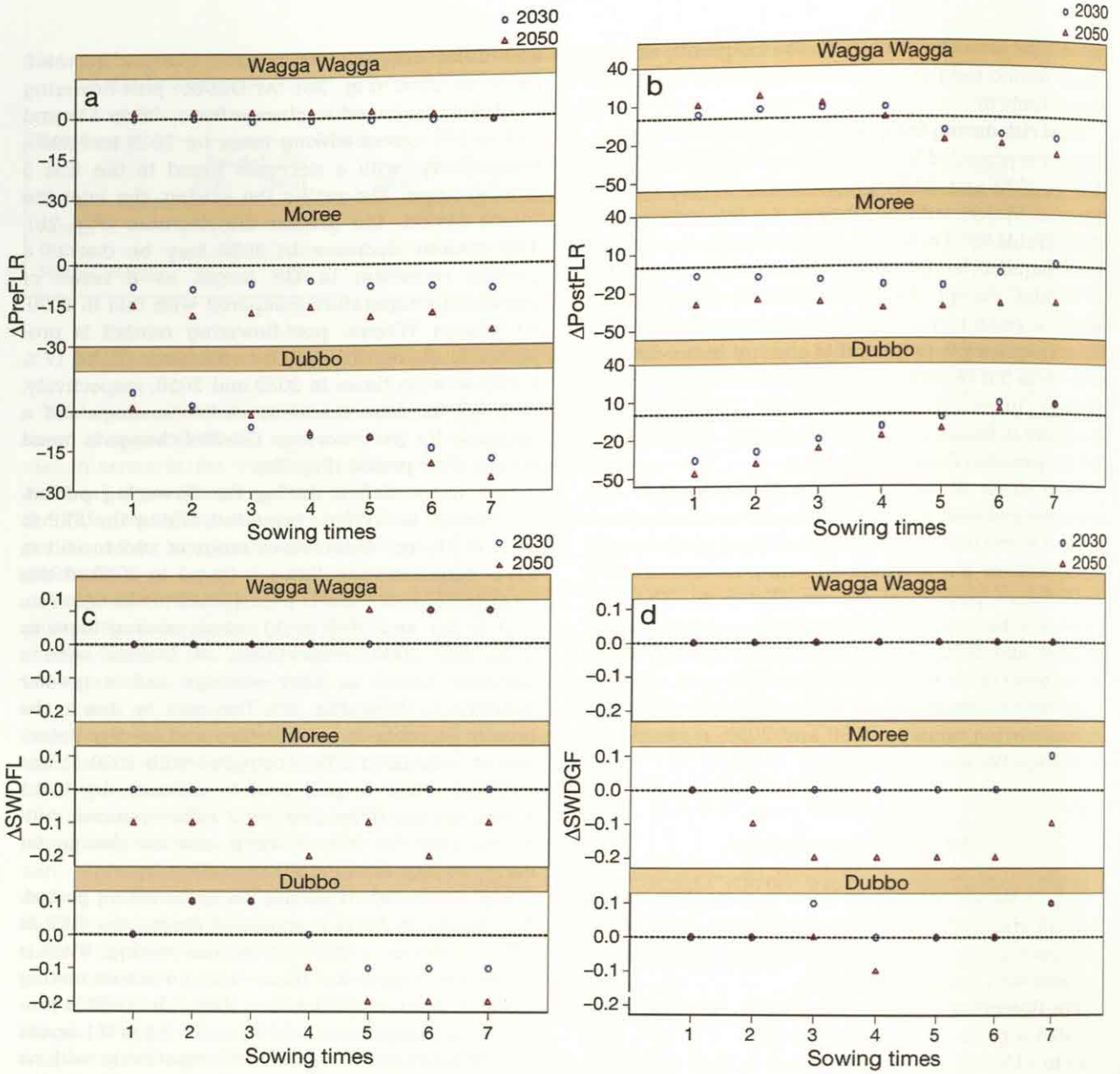

Fig. 2. Multi-model ensemble mean changes in (a) pre- and (b) post-flowering rainfall (%) and soil water deficit (absolute change without unit) during (c) flowering and (d) grain filling periods across sowing times, locations and future periods (2030, 2050), compared with the baseline situation. Abbreviations as in Table 4

last 5 sowing times in 2030 and 2050, respectively, with the greatest increase associated with the 3rd sowing, indicating the optimum sowing time under future climate-change conditions (Fig. 3). No change in wheat yield across sowing times is projected at Wagga Wagga in 2030, except for the last sowing, when an increase of 1% is found. Small increases (1–2%) in wheat grain yield in 2050 across sowing times is projected at Wagga Wagga (Fig. 3).

4. DISCUSSION

4.1. Temperature-related risk

Different production areas and sowing times are likely to have different responses to a warmer environment in the frequency of frost occurrence during both FLP and GFP (Table 6). This is in line with the findings of Zheng et al. (2012), who reported spatial variability in the occurrence of frost events across the

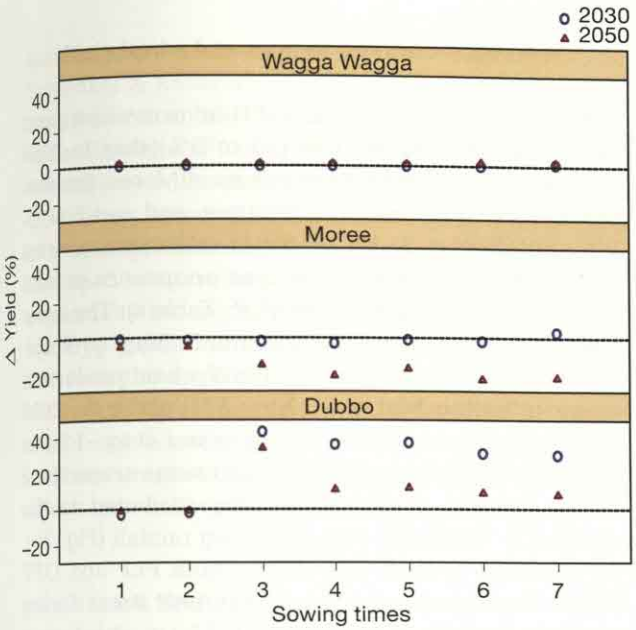

Fig. 3. Multi-model ensemble mean changes in wheat grain yield across sowing times, locations and future periods (2030, 2050), compared with the baseline situation

Australian wheat belt. The change in sign (decrease or increase) in the frequency of frost occurrence is determined by the effects of increased temperature on crop development (crops develop more rapidly in a warmer environment, exposing them to cooler conditions, and thus a higher frost risk) and the direct effects of increased temperature on frost occurrence (reduced occurrence of frost). The former observation is supported by previous studies and illustrated in Fig. 4. The start of flowering would be advanced 4–7 d in 2030 and 5–11 d in 2050 across sowing times and locations (Fig. 4). Zheng et al. (2012), Anwar et al. (2015) and Yang et al. (2014) also reported substantial advancement of wheat phenology, including the time of flowering, in a warmer environment. The greater decrease in frost frequency in a warmer environment at Wagga Wagga (Table 6) is due to a lower existing temperature regime (Table 1) compared with the other 2 locations.

The later the future period, the more the frequency of heat stress increased during FLP across sowing times and locations (Table 6). The greater increase in heat stress at Moree and Dubbo is due to higher existing temperatures (Table 1) and a greater increase in maximum temperature (Table 5) compared with that at Wagga Wagga. Semenov (2007) found that heat-waves during wheat flowering are likely to substantially increase in magnitude and frequency at Rothamsted, UK. Holzkämper et al. (2013) also reported an increase in heat stress in Switzerland under climate-change scenarios. An increase in frost risk during the GFP is because the effects of increased temperature on crop development (crops develop more rapidly in a warmer environment, exposing them to colder conditions, hence leading to higher frost risk; Fig. 4) outweighed the effects of increased temperature on minimum temperature (reduced ocurrence of frost). Similarly, decreases in the frequency of heat stress during the GFP are, in some cases, because the effects of increased temperature

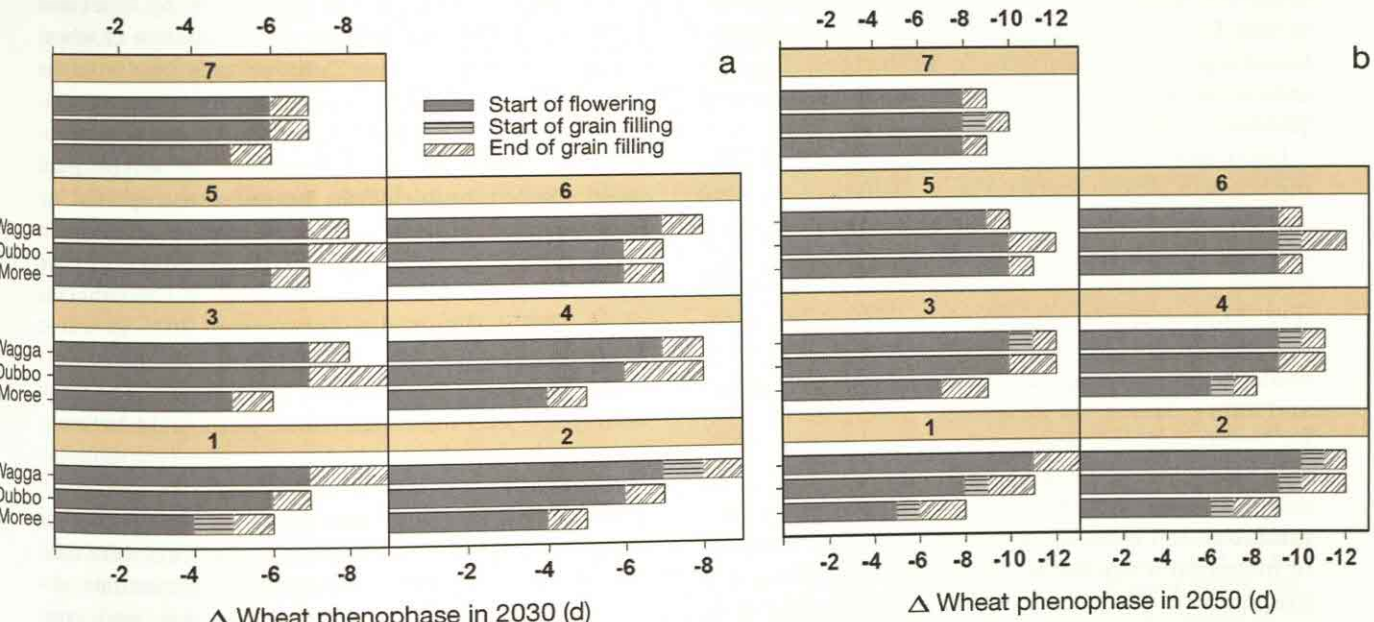

Fig. 4. Multi-model ensemble mean changes in wheat phenophases in 2030 (a) and 2050 (b) across sowing times and locations compared with the baseline situation

on crop development (bringing crops to a cooler environment; Fig. 4) outweighed the effect of increased temperature on the occurrence of heat stress.

4.2. Rainfall-related risk

The present study reported a change in the range of pre- and post-flowering rainfall of from −9 to −6% and −15 to 2%, respectively, in 2030 under the A2 emission scenario (Fig. 2a,b). Terminal drought and heat stress during reproductive stages are major constraints on current wheat production in Southeast Australia (Cawood 1996). A decrease in post-flowering rainfall (Fig. 2b) (especially at Moree and Dubbo) and the increased chance of heat stress during FLP and GFP (Table 6) imply that these 2 existing problems would be exacerbated in a changing climate. Deteriorating agro-climatic conditions under future climate change were also reported by Trnka et al. (2011). Hence, effective adaptation strategies need to be identified (e.g. breeding heat- and drought-tolerant cultivars) and implemented for maintaining/enhancing the current wheat production level in order to deal with future climate change.

Even though an increase in post-flowering rainfall are projected with the last 2 sowings at Dubbo (Fig. 2b), late sowings normally lead to a lower grain yield due to the reduced GS length for biomass accumulation. This means that increases in post-flowering rainfall may not compensate for yield reduction due to delayed sowing. Unlike Moree and Dubbo, an increase in post-flowering rainfall at Wagga Wagga would be found with early sowings (the first 4 sowings) (Fig. 2b), indicating opportunities exist for enhancing wheat yield in a changing climate at this location.

Decreases in SWD during FLP and GFP across sowing times in 2050 at Moree (Fig. 2c,d) indicate a more stressful soil water status. This reflected the greater increase in seasonal temperature (Table 5) and greater reduction in seasonal rainfall in 2050 (Fig. 2a,b) compared with those in 2030 at this location. Similar findings were also reported by Rivington et al. (2013) regarding SWD in the context of Scotland and future climate. An increase in SWD (less soil water stress) during FLP and GFP across study periods and some sowing times at Dubbo (Fig. 2c,d) may be due to the fact that the positive effects of increased rainfall on soil water outweighed the negative effects of increased temperature on soil water (e.g. via soil evaporation). The same is true for the increase in SWD during the FLP, with later sowings across both future periods at Wagga Wagga (Fig. 2c).

4.3. Agro-climatic indices and wheat yield

The range and magnitude of change in wheat grain yield was smaller in 2030 (−3 to 3%) than in 2050 (−23 to −5%) across sowing times at Moree; this was due to (1) less decrease in both pre- and post-flowering rainfall (Fig. 2a,b), (2) better soil moisture status (Fig. 2c,d) and (3) less frequent occurrence of heat stress, especially during the FLP (Table 6). The latter change in range is in line with the findings by Potgieter et al. (2013) for northern NSW wheat production areas including Moree (−30 to −5%) under the 2050 high emission scenario. A decrease (−3 to −1%) in wheat grain yield for the first 2 sowings across the 2 future periods at Dubbo can be attributed to the greatest decrease in post-flowering rainfall (Fig. 2b), an increase in frost risk during both FLP and GFP (Table 6) and a greater increase in heat stress during the FLP (Table 6). An increase (0–2%) in wheat grain yield in 2050 across sowing times compared with flowering rainfall at Wagga Wagga (Fig. 2a). A change of −6 to 5% in wheat yield was reported by Potgieter et al. (2013) for southern NSW wheat production areas, including Wagga Wagga, under the 2050 high emission scenario, which encompasses the findings of the present study (0–2%) for the 2050 period. Spatial difference in wheat yield change was reported by Yang et al. (2014). Their study reported a change in the yield range of −14.7 to 3.4% in 2030 across wheat growing regions in the NSW wheat belt compared to a change of −3 to 43% from the present study for the same period across sowing times and study locations. Differences in the change of wheat yield ranges from these 2 studies may be due to the different sowing times and study locations considered and the different GCMs and downscaling approaches used. Spatial differences in wheat grain yield due to high-degree hours were reported by Innes et al. (2015): greater reduction in wheat grain yield (−15% on average) was found in the warmer and drier north-western shires of NSW. Ummenhofer et al. (2015) reported a decrease of 70% in wheat grain yield by the late 21st century for southeast Australia, including the southern NSW region. The large difference in projected wheat grain yield between their study and the present study can be attributed to (1) the different time horizons considered (end vs. early and middle periods of this century), (2) whether or not enhanced CO_2 physiological effects were considered and (3) the different emission scenarios, climate models, downscaling approaches and crop models used. It should be noted that enhanced CO_2 may have offset the negative effects of increased

temperature- and rainfall-related climate risks. Schlenker & Roberts (2009) reported that crop yield would decrease 30–46% and 63–82%, respectively, under B1 and A1F1 emission scenarios by the end of this century without the consideration of enhanced CO_2. Using later maturity cultivars may be an effective strategy in mitigating the negative effect of increased temperature on shortened GS length (less opportunity for crops to accumulate biomass, hence low crop yield). Identifying the optimal sowing time and selecting appropriate wheat cultivars (to match the sowing time) to ensure a safe flowering window would significantly reduce the occurrence of frost and heat stress at this critical stage and their ensuing effects on wheat crop yield.

4.4. Study features and limitations

This study has a number of features. (1) The use of downscaled daily outputs of multiple GCMs, which allowed the analysis of extreme climate events in relation to wheat production systems such as the frequency of frost and heat stress during key phenophases. It is widely recognised that large climate model-to-model difference exists. To overcome this issue, multi-model ensemble mean changes in climate, agro-climate indices and yield were used. (2) The assessment of cultivar- and sowing-time-specific agro-climate indices under future climate scenarios. (3) This study extended agro-climate index assessment to yield assessment, which has not been done in previous studies on this topic. Caution must be taken with the simulated results, as significant differences exist in some of the agro-climatic indices associated with specific locations (Table 4). Mavromatis & Hansen (2001) and Qian et al. (2004) pointed out that LARS-WG has a limited ability to reproduce interannual climate variability. This was confirmed by the present study (Fig. 1).

5. CONCLUSIONS

Adverse agricultural environments (e.g. an increase in the frequency of heat stress during wheat flowering and grain filling periods, and a decrease in pre- and post-flowering rainfall) were projected for the 2030 and 2050 periods at the 3 locations considered in this study. The concurrent occurrence of heat stress and terminal drought at wheat reproductive stages could pose a significant challenge for the sustainable development of the wheat industry in the future, especially at Moree, where the existing temperature is already higher than that at the other 2 locations. This implies that effective plant breeding and management strategies (e.g. optimising sowing time to match appropriate wheat cultivars, the breeding and use of frost-, heat- and drought-tolerant cultivars, soil water conservation practices) need to be put into place to deal with the increased climate risks at critical stages of wheat crops under changing climatic conditions.

Acknowledgements. The author would like thank Dr Semenov, Rothamsted Research, UK, for providing the weather generator: LARS-WG and Dr John McGregor, CSIRO Marine and Atmospheric Research, Australia, for providing the daily outputs of CCAM used in this study.

LITERATURE CITED

Anwar MR, Liu DL, Farquharson R, Macadam I and others (2015) Climate change impacts on phenology and yield of five broadacre crops at four climatologically distinct locations in Australia. Agric Syst 132:133–144

Cawood R (1996) Principals of sustainable agriculture: climate, temperature and crop production in south-eastern Australia. Victorian Institute for Dryland Agriculture, Horsham, VIC

CSIRO and BoM (Commonwealth Scientific and Industrial Reasearch Organization and Bureau of Meteorology) (2007) Climate change in Australia, Technical report. www.climatechangeinaustralia.gov.au (accessed 20 March 2016)

CSIRO and BoM (2014) State of the climate. www.bom.gov.au/state-of-the-climate/ (accessed 20 March 2016)

Cubasch U, Meehl GA, Boer GJ, Stouffer RJ and others (2001) Projections of future climate change. In: Houghton JT, Ding Y, Griggs DJ, Noguer M and others (eds) Climate change 2001: the scientific basis. Contribution of Working Group I to the 3rd assessment report of the Intergovernmental Panel on Climate Change. Cambridge University Press, Cambridge, p 525–582

Fuller MP, Fuller AM, Kaniouras S, Christophers J, Fredericks T (2007) The freezing characteristics of wheat at ear emergence. Eur J Agron 26:435–441

GRDC (Grains Research and Development Corporation) (2014) GroundCover—research to profit grain growers: Southern Region 109. GRDC, Canberra

Holzkämper A, Calanca P, Fuhrer J (2013) Identifying climatic limitations to grain maize yield potentials using a suitability evaluation approach. Agric For Meteorol 168: 149–159

Holzworth DP, Huth NI, deVail PG, Zurcher EJ and others (2014) APSIM—evolution towards a new generation of agricultural systems simulation. Environ Model Softw 62: 327–350

Innes PJ, Tan DKY, Van Ogtrop F, Amthor JS (2015) Effects of high-temperature episodes on wheat yield in New South Wales, Australia. Agric For Meteorol 208:95–107

IPCC (Intergovernmental Panel on Climate Change) (2000) Emissions scenarios. Special report of the IPCC. Cambridge University Press, Cambridge

Liu DL, Timbal B, Mo JH, Fairweather H (2011) A GIS-based climate change adaptation strategy tool. Int J Clim Chang Strateg Manag 3:140–155

Luo Q, Kathuria A (2013) Modelling the response of wheat grain yield to climate change: a sensitivity analysis. Theor Appl Climatol 111:173–182

Luo Q, Wen L (2015) The role of climatic variables in winter cereal yield: a retrospective analysis. Int J Biometeorol 59:181–192

Luo Q, Williams M, Bellotti WD, Bryan B (2003) Quantitative and visual assessment of climate change impacts on South Australian wheat production. Agric Sys 77:173–186

Luo Q, Bellotti WD, Hayman P, Williams M, Devoil P (2010) Effects of changes in climatic variability on agricultural production. Clim Res 42:111–117

Luo Q, Wen L, McGregor JL, Timbal B (2013) A comparison of downscaling techniques in the projection of local climate change and wheat yield. Clim Change 120:249–261

Luo Q, Bange M, Clancy L (2014) Cotton phenology in a new temperature regime. Ecol Modell 285:22–29

Matthews P, McCaffery D (2012) Winter crop variety sowing guide 2012. New South Wales Department of Primary Industries, Orange, NSW

Mavromatis T, Hansen JW (2001) Interannual variability characteristics and simulated crop response of four stochastic weather generators. Agric For Meteorol 109: 283–296

McGregor JL, Dix MR (2008) An updated description of the Conformal-Cubic Atmospheric Model. In: Hamilton K, Ohfuchi W (eds) High resolution simulation of the atmosphere and ocean. Springer, Heidelberg, p 51–76

O'Leary G, Christy B, Nuttall J, Huth N and others (2015) Response of wheat growth, grain yield and water use to elevated CO_2 under a Free Air CO_2 Enrichment (FACE) experiment and modelling in a semi-arid environment. Glob Change Biol 21:2670–2686

Porter JR, Gawith M (1999) Temperatures and the growth and development of wheat: a review. Eur J Agron 10:23–36

Potgieter A, Meinke H, Doherty A, Sadras VO, Hammer G, Crimp S, Rodriguez D (2013) Spatial impact of projected changes in rainfall and temperature on wheat yield in Australia. Clim Change 117:163–179

Qian B, Gameda S, Hayhoe H, De Jong R, Bootsma A (2004) Comparison of LARS-WG and AAFC-WG stochastic weather generators for diverse Canadian climates. Clim Res 26:175–191

Rivington M, Matthews KB, Buchan K, Miller DG, Bellocchi G, Russell G (2013) Climate change impacts and adaptation scope for agriculture indicated by agro-meteorological metrics. Agric Syst 114:15–31

Schlenker W, Roberts MJ (2009) Nonlinear temperature effects indicate severe damages to U.S. crop yield under climate change. Proc Natl Acad Sci USA 106:15594–15598

Semenov MA (2007) Development of high-resolution UKCIP02-based climate change scenarios in the UK. Agric For Meteorol 144:127–138

Semenov MA (2008) Simulation of extreme weather events by a stochastic weather generator. Clim Res 35:203–212

Semenov MA, Brooks RJ, Barrow EM, Richardson CW (1998) Comparison of the WGEN and LARS-WG stochastic weather generators in diverse climates. Clim Res 10: 95–107

Thorburn P, Hochamn Z, Chapman S, Zheng B (2013) The approach to representing temperature effects in APSIM-Wheat (v7.4). In: Proc Workshop 'Modelling wheat response to high temperature'. CIMMYT, El Batan, p 43–46

Trnka M, Olesen JE, Kersebaum KC, Skjelvag AO and others (2011) Agroclimatic conditions in Europe under climate change. Glob Change Biol 17:2298–2318

Ummenhofer CC, Xu H, Twine TE, Girvetz EH, McCarthy HR, Chhetri N, Nicholas KA (2015) How climate change affects extremes in maize and wheat yield in two cropping regions. J Clim 28:4653–4687

Wang B, Liu DL, Asseng S, Macadam I, Yu Q (2015) Impact of climate change on wheat flowering time in eastern Australia. Agric For Meteorol 209–210:11–21

Weigel AP, Liniger MA, Appenzeller C (2008) Can multimodel combination really enhance the prediction skill of probabilistic ensemble forecasts? QJR Meteorol Soc 134: 241–260

Wheeler TR, Batts GR, Ellis RH, Hadley P, Morison JIL (1996) Growth and yield of winter wheat (*Triticum aestivum*) crops in response to CO^2 and temperature. J Agric Sci 127:37–48

Wheeler TR, Craufurd PQ, Ellis RH, Porter JR, Vara Prasad PV (2000) Temperature variability and the yield of annual crops. Agric Ecosyst Environ 82:159–167

Yang YM, Liu DL, Anwar MR, Zuo HP, Yang YH (2014) Impact of future climate change on wheat production in relation to plant-available water capacity in a semiarid environment. Theor Appl Climatol 115:391–410

Zheng B, Chenu K, Dreccer MF, Chapman SC (2012) Breeding for the future: What are the potential impacts of future frost and heat events on sowing and flowering time requirements for Australian bread wheat (*Triticum aestivium*) varieties? Glob Chang Biol 18:2899–2914

Editorial responsibility: Gerrit Hoogenboom, Gainesville, Florida, USA

Submitted: August 17, 2015; Accepted: April 28, 2016
Proofs received from author(s):June 16, 2016